Shape-Persistent Macrocycles: Building Blocks for Complex Organic and Polymeric Architectures

Sigurd Höger, Klaus Bonrad, Silvia Rosselli, Anne-Désirée Ramminger, Thomas Wagner, Beate Silier, Simone Wiegand, Wolfgang Häußler, Günter Lieser, Volker Scheumann*

Max Planck Institute for Polymer Research, Ackermannweg 10, 55128 Mainz, Germany

Summary: Alkyl- and Oligostyrene substituents were attached to shape-persistent macrocycles based on a phenyl-ethynyl backbone. In good solvents for both the rigid core and the flexible corona no aggregation occurred. Whereas, addition of a solvent that selectively solubilizes the corona induced a solvophobic aggregation. For alkyl substituted rings the experimental data were described by a monomer-dimer equilibrium. In contrast, the oligostyrene substituted rings formed more expanded aggregates which were investigated by scattering and by imaging methods. The superstructures are consequently described as hollow supramolecular cylindrical brushes.

Introduction

Shape-persistent macrocycles based on the rigid phenyl-ethynyl backbone are readily obtainable in good to high yields by the oxidative Glaser coupling of the corresponding bisacetylenes. These couplings can be performed either in a statistical approach (Fig. 1a) or by using templates (Fig. 1b)[1].

Attachment of alkyl or oligoalkyl groups to the macrocycles leads to structures that exhibit an essentially two dimensional conformation (Fig. 2). Proton NMR spectra of **1** in THF or CH_2Cl_2 do not show any concentration dependence, and therefore, give no indication for ring aggregation. This result is not surprising because there are no highly polar groups in the molecule that could induce such aggregation. In addition, the size of the π-system relative to the extension of the molecule is rather small, and aggregation of large macrocycles has been reported only for compounds having electron withdrawing groups[2].

 CCC 1022-1360/00/$ 17.50+.50/0

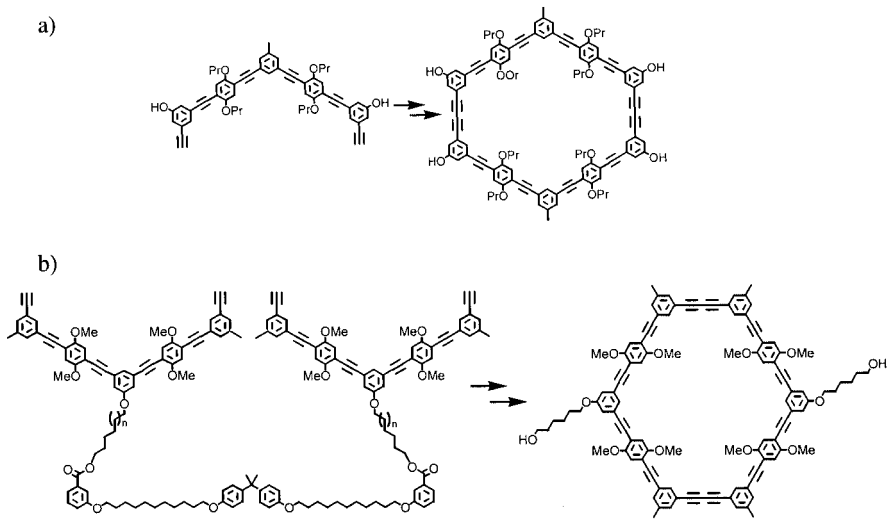

Fig. 1: Synthesis of functionalized shape-persistent macrocycles by the Glaser coupling: a) statistical approach; b) template approach.

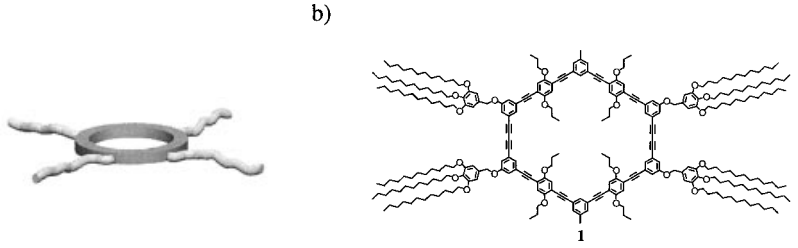

Fig. 2: Oligoalkyl substituted macrocycles: a) schematic; b) structure of **1**.

Macrocycle Aggregation

In a solvent mixture of CH_2Cl_2 and *n*-hexane, however, a strong concentration dependence of the NMR signals is observed. Assuming a monomer-dimer equilibrium as the predominant association process in solution, the dimerization constant increases from $K_D = 130 \pm 30\ M^{-1}$ (in CD_2Cl_2/hexane (1:3) at 25 °C) to $K_D = 790 \pm 180\ M^{-1}$ (in CD_2Cl_2/hexane (1:6) at 25 °C) by increasing the volume fraction of hexane[3]. These data indicate that aggregation of the oligoalkyl substituted macrocycles can be facilitated by the addition of a solvent that acts as a good solvent for the peripheric alkyl chains and as a poor solvent for the core (i.e.,

solvophobically induced aggregation, Fig. 3)[4]. It must be pointed out, however, that a further increase of the association constants of **1** by increasing the volume fraction of the non polar solvent is not possible due to the limited compound solubility in hexane.

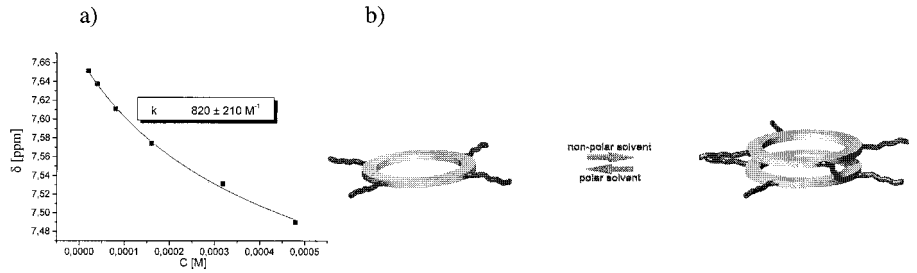

Fig. 3: Aggregation of oligoalkyl substituted shape-persistent macrocycles: a) concentration dependent chemical shift of one aromatic proton of **1**; b) schematic description of a monomer-dimer equilibrium.

A simple way to overcome this problem is the attachment of short, non-crystallizable oligomeric side groups to the ring. DCC-coupling of the corresponding macrocyclic diol and narrow-distributed (PD (M_w/M_n) < 1.1) polystyrene carboxylic acid oligomers of different molecular weight (M_w: 1000(**a**), 1500(**b**), 2500(**c**); 3500(**d**); 5000(**e**) g/mol) produces the products **2a-e** in good yields (70 - 90 %)[5]. The resulting structures can be described as coil-(rigid)ring-coil block copolymers, a subclass of rod-coil block copolymers, which are known to microphase separate to well-ordered superstructures even at relatively small block sizes[6]. Due to the coiled conformation of the side groups, these molecules have an extension in the third dimension (Fig. 4).

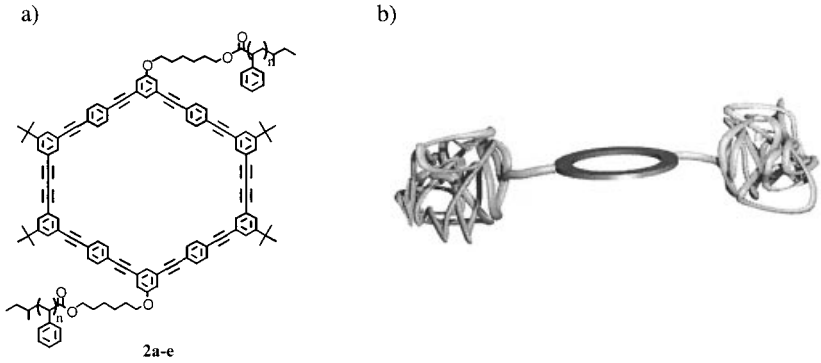

Fig. 4: Oligostyrene substituted macrocycles: a) structure of **2**; b) schematic.

2a-e are readily soluble at room temperature in chloroform, dichloromethane, THF and toluene. In addition **2b-e** are soluble in warm cyclohexane. Upon cooling, **2b** forms a gel at concentrations above 0.5 wt %. Under the same conditions **2c** rapidly forms a very viscous solution, as does **2d** after several days. These solutions are also strongly birefringent with the exception of solutions of **2e**, which exhibit neither unusual viscosity nor birefringence.

As for **1**, these observations can be explained by the different solubility of the rigid cyclic block and the flexible oligostyrene block of the copolymer **2**. Cyclohexane is a solvent for polystyrene but, in contrast to THF or toluene, a non-solvent for the unsubstituted macrocycle. The attachment of the polymeric side groups, even of relatively low molecular weight, is sufficient enough to solubilize the block copolymer in the non-polar cyclohexane at elevated temperatures. Upon cooling, the rigid parts of the block copolymer aggregate if the size of the coiled blocks is below a certain level. As expected, extension and aggregation kinetics strongly depend on the block size of the polystyrene.

Dynamic light scattering (DLS) was performed on solutions of **2c** in toluene and cyclohexane to investigate its aggregation behaviour in more detail. The distribution of the relaxation times in the autocorrelation functions were obtained by CONTIN analysis. As expected, in toluene (0.11 wt %) only one maximum that corresponds to a hydrodynamic radius of approximately 2 nm is found. This maximum corresponds to the size of a simple block copolymer molecule **2c**. In contrary, the light scattering data in cyclohexane at the same concentration showed the formation of more complex structures. The elaboration of the measured autocorrelation function resulted in a distribution of relaxation times that contain two maxima, one at approximately 2 nm and the other at approximately 60 nm (Fig. 5a).

a) CONTIN fit

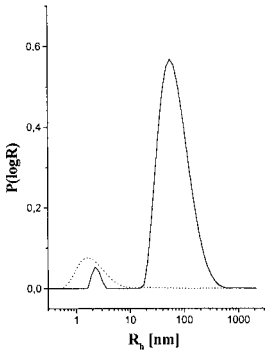

b) Kratky plot

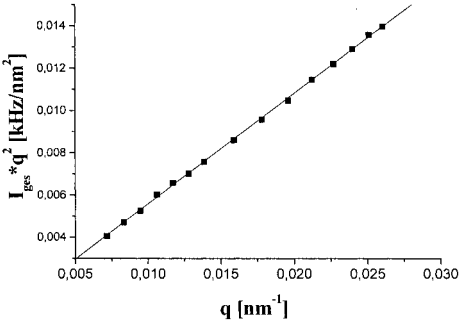

Fig 5: a) CONTIN-fit: rate distribution of **1c** in toluene (·····) and in cyclohexane (—) at a concentration of 0.11 wt %; b) Kratky plot for the slow mode of **2c** in cyclohexane (■) at a concentration of 0.09 wt % and linear data fit (—).

With increasing concentration the fraction of the larger species increases. The angle dependence of the scattered light intensity of the larger objects (Fig. 2b) suggested the presence of rod-shaped objects with a high virtual persistent length of more than 100 nm and a total length of about 250 nm to 1200 nm[7]. The diameter of these cylindrical objects was determined by ultra small angle X-ray scattering (USAXS) and small angle X-ray scattering (SAXS) in cyclohexane (2 wt %) (Fig. 6).

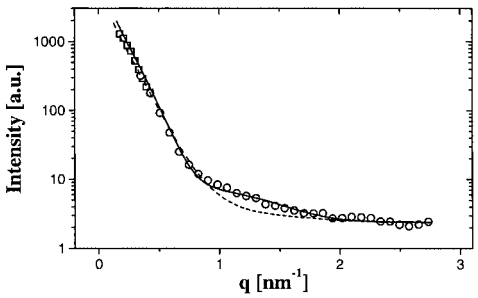

Fig. 6: USAXS (□)-SAXS (○) data of a 2.0 wt % cyclohexane solution of **1c**. The lines represent the form factor for a massive cylinder (----) with a external diameter of 10 ± 3.8 nm, and for a hollow cylinder (——) with an external diameter of 10 ± 3.8 nm and an internal diameter of 1.8 ± 0.5 nm.

The description of the measured data was not possible by using a simple massive cylinder model (showing an abrupt radial electron density change) of any length or thickness. The different length of the oligomeric polystyrene chains and the radial decrease of the cylinder density was therefore taken into account by giving the cylinder a polydispersity with respect to the diameter. The calculated form factor of a massive cylinder 10 nm in diameter having a polydispersity at the outside (d_{out} = 10 nm, polydispersity: 3.8 nm, half width half maximum of a Gaussian distribution) agrees with the observed data at low q-values. However, the observed scattering intensity is remarkably higher than the theoretical prediction in the q-range between 1 and 2 nm^{-1}. Only the use of a radial density profile with a reduced electron density inside the cylinder resolved this discrepancy. The calculated form factor of a cylinder with the same electron density profile at the outside as described before and with an additional reduced electron density at the inside (hollow size d_{in} = 1.8 nm, polydispersity: 0.5 nm, half width half maximum of a Gaussian distribution) fits with the observed data over the entire q-range. The scattering data undoubtedly show that the coil-ring-coil block copolymers aggregate in solution into *hollow* cylinder-shaped objects with a high virtual persistent length (Fig. 7).

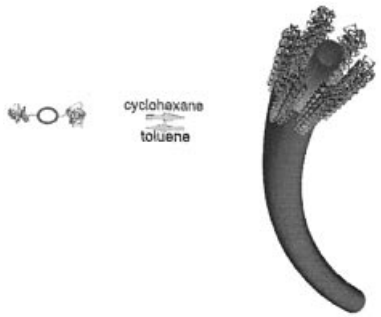

Fig. 7: Schematic aggregation of oligostyrene substituted shape-persistent macrocycles.

Independent evidence of these supramolecular cylinders was obtained by using imaging methods. The transmission electron micrograph (TEM) of a sample obtained by freeze-drying a cyclohexane solution (Pt/C shadowed film) shows ribbons of different width at the sample surface, the narrowest in the range of approximately 15 nm (Fig. 8a).

a) TEM picture b) AFM picture

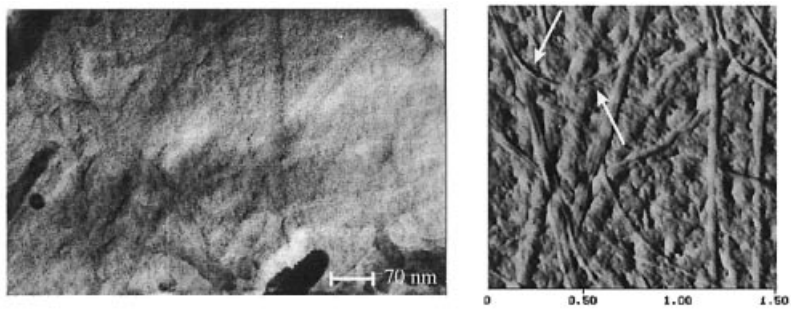

Fig. 8: a) TEM of a C/Pt shadowed film obtained by freeze drying a 0.15 wt % cyclohexane solution of **2c**; b) AFM (amplitude picture, 1.5 × 1.5 μm^2): Film obtained by dipping mica into a 0.15 wt % cyclohexane solution of **2c**.

Atomic force microscopy (AFM) images of a polymer film on mica show long bundles of two or three cylindrical aggregates, together with individual aggregates (Fig. 8b). Taking in consideration the width of the AFM tip, the cylindrical units have a diameter of approximately 10-15 nm. The dimensions obtained by TEM and AFM correspond well with the molecular dimensions obtained by scattering methods and are in accordance with the molecular dimensions of the molecular building blocks[8]. Surveying the most curved cylindrical object found in the AFM images (white arrows, Fig. 8b) and treating it as worm-like chain results in

a persistent length of approximately 350 nm of the cylindrical aggregate. The correspondence of these structures with covalently linked polymer brushes suggests that they can be described as hollow supramolecular cylindrical brushes[9].

Conclusion

It has been shown that shape-persistent macrocycles containing solubilizing side groups can aggregate in solvents or solvent mixtures that selectively dissolve the corona of the rings and act as non-solvents for the rigid core. While oligoalkyl substituted rings form predominantly dimers, rings with oligostyrene substituents can aggregate to large hollow supramolecular cylinders. These have been investigated by scattering methods and could be visualized by electron microscopy and atomic force microscopy.

1. Reviews about shape-persistent macrocycles: J. S. Moore, *Acc. Chem. Res.* **30**, 402 (1997); S. Höger, *J. Polym. Sci. Part A*, **37**, 2685 (1999); M. M. Haley, J. J. Pak, S. C. Brand, *Topic Curr. Chem.* **201**, 81 (1999)
2. J. Zhang, J. S. Moore, *J. Am. Chem. Soc.* **114**, 9701 (1992); A. S. Shetty, J. Zhang, J. S. Moore, *J. Am. Chem. Soc.* **118**, 1019 (1996); Y. Tobe, N. Utsumi, K. Kawabata, K. Naemura, *Tetrahedron Lett* **37**, 9325 (1996); Y. Tobe, N. Utsumi, A. Nagano, K. Naemura, *Angew. Chem. Int. Ed. Engl.* **37**, 1285 (1998)
3. R. B. Martin, *Chem. Rev.* **96**, 3043 (1996). The supramolecular polymerization in solution can be described by the same model. Therefore, by analyzing the NMR data alone, we can not discriminate between dimers and polymers of the oligo-alkyl substituted rings
4. S. Höger, K. Bonrad, A. Mourran, U. Beginn, M. Möller, *J. Am. Chem. Soc.* **123**, 5651 (2000)
5. S. Rosselli, A.-D. Ramminger, T. Wagner, B. Silier, S. Wiegand, W. Häußler, G. Lieser, V. Scheumann, S. Höger, *Angew. Chem. Int. Ed. Engl.* in print
6. E. R. Zubarev, M. U. Pralle, L. Li, S. I. Stupp, *Science* **283**, 523 (1999); J. T. Chen, E. L. Thomas, C. K. Ober, G.-P. Mao, *Science* **273**, 343 (1996); S. A. Jenekhe, X. L. Chen, *Science* **283**, 372 (1999); M. Lee, B.-K. Cho, H. Kim, W.-C. Zin, *Angew. Chem. Int. Ed. Engl.* **37**, 638 (1998); M. Muthukumar, C. K. Ober, E. L. Thomas, *Science* **277**, 1225 (1997); H. Engelkamp, S. Middelbeek, R. J. M. Nolte, *Science* **284**, 785 (1999); H.-A. Klok, J. F. Langenwalter, S. Lecommandoux, *Macromolecules* **33**, 7819 (2000)
7. For the estimation of the rod length L from R_h, the relation $R_g/R_h = 2$ was used (valid for rod-like object such as fibrinogen or TMV). With $R_g^2 = L^2/12$ follows $L = [12\ (2R_h)^2]^{1/2}$; H.-G. Elias, *Makromoleküle Bd. 1* (Verlag Hüthig & Wepf, Basel, 1990)
8. S. Höger, V. Enkelmann, *Angew. Chem. Int. Ed. Engl.* **34**, 2713 (1995); S. Höger, V. Enkelmann, K. Bonrad, C. Tschierske, *Angew. Chem. Int. Ed. Engl.* **39**, 2268 (2000)
9. P. Dziezok, S. S. Sheiko, K. Fischer, M. Schmidt, M. Möller, *Angew. Chem. Int. Ed. Engl.* **36**, 2812 (1997); A. D. Schlüter, J. P. Rabe, *Angew. Chem. Int. Ed. Engl.* **39**, 864 (2000)